ISSN 0001-4370, Oceanology, 2017, Vol. 57, No. 4, pp. 593–599. © Pleiades Publishing, Inc., 2017.
Original Russian Text © S.Yu. Sokolov, E.A. Moroz, A.S. Abramova, Yu.A. Zarayskaya, K.O. Dobrolubova, 2017, published in Okeanologiya, 2017, Vol. 57, No. 4, pp. 655–662.

INSTRUMENTS AND METHODS

# Mapping of Sound Scattering Objects in the Northern Part of the Barents Sea and Their Geological Interpretation

**S. Yu. Sokolov*, E. A. Moroz, A. S. Abramova, Yu. A. Zarayskaya, and K. O. Dobrolubova**

*Geological Institute, Russian Academy of Sciences, Moscow, Russia*

**e-mail: sysokolov@yandex.ru*

Received December 17, 2015; in final form, March 30, 2016

**Abstract**—On cruises 25 (2007) and 28 (2011) of the R/V *Akademik Nikolai Strakhov* in the northern part of the Barents Sea, the Geological Institute, Russian Academy of Sciences, conducted comprehensive research on the bottom relief and upper part of the sedimentary cover profile under the auspices of the International Polar Year program. One of the instrument components was the SeaBat 8111 shallow-water multibeam echo sounder, which can map the acoustic field similarly to a side scan sonar, which records the response both from the bottom and from the water column. In the operations area, intense sound scattering objects produced by the discharge of deep fluid flows are detected in the water column. The sound scattering objects and pockmarks in the bottom relief are related to anomalies in hydrocarbon gas concentrations in bottom sediments. The sound scattering objects are localized over Triassic sequences outcropping from the bottom. The most intense degassing processes manifest themselves near the contact of the Triassic sequences and Jurassic clay deposits, as well as over deep depressions in a field of Bouguer anomalies related to the basement of the Jurassic–Cretaceous rift system

**DOI:** 10.1134/S000143701704018X

## INTRODUCTION

The use of multibeam echo sounders for detailed mapping of bottom relief has led to breakthroughs in geomorphology, tectonics, and the geology of oceanic and shelf territories. The introduction of multibeam echo sounders that can record the acoustic field similar to a side scan sonar (SSS) has made it possible with one device to collect different types of hydroacoustic information without taking into account the separate geometry of the devices with synchronous spatial matching of both datasets. Sonogram processing has shown that in addition to the characteristics of the bottom properties, the given instrument base yields information on the current distribution of acoustically contrasting properties of the water column. Mapping of sound scattering objects (SSOs) allows their joint interpretation with bottom structures, which broadens the cognitive possibilities of information obtained by marine underwater equipment. There are various methods for collecting, processing, visualizing, and interpreting data. Here, we present the simple method of mapping SSOs in the water column during reconnaissance surveys. We used materials obtained by the Geological Institute, Russian Academy of Sciences, from the R/V *Akademik Nikolai Strakhov* on cruises 25 (2007) and 28 (2011) under the auspices of the International Polar Year program. Operations were conducted on the north side of the Barents Sea depression near the Franz Joseph Land archipelago using a system of sublatitudinal legs. The goal of the expedition was to study the structure of the upper part of the profile for this area. During operations, significant accumulations of SSOs were detected in the water column, the origin of which was interpreted as deep degassing, rather than accumulations of biological objects. This study explains the methods for processing and interpreting the origin of sonar anomalies in the water column. Note that the possible origin of gases forming SSOs in the water column is discharge of fluid from disintegrating sediment due to the disrupted integrity of supporting fluid: lithological or physical (gas hydrate sole). The direct supply of fluid from deep zones of the North Barents Depression located in the catagenetic temperature interval, or any other reasons, is not discussed. The authors stress that SSOs are formed by fluid discharges from the bottom and that this can be concluded based on the spatial distribution of SSOs constructed using the proposed technique and its comparison with independent geological data.

## DATA PROCESSING TECHNIQUE

When surveying the bottom relief with a multibeam echo sounder, devices with frequencies of 100–400 kHz for shallow-water areas and 12–25 kHz for deep-water areas are used. Reflected (near the central beam) and scattered acoustic fields are detected with a phased array, which forms a set of beams within the limits of

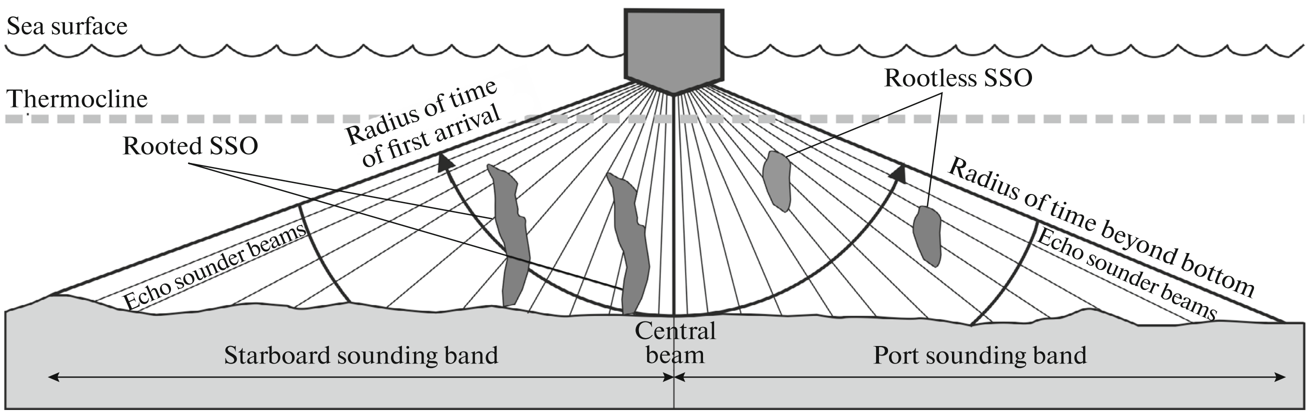


**Fig. 1.** Main concepts and geometry of data during multibeam echo sounding.

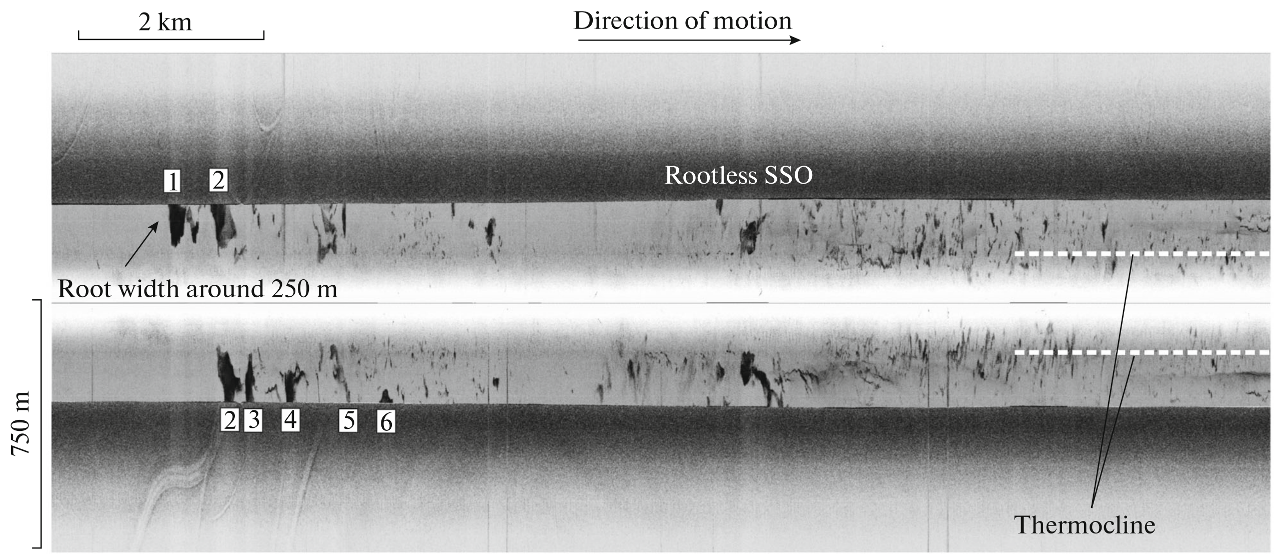


**Fig. 2.** Example of recording of sonar data from echo sounder with rootless and rooted SSOs without correction of signal for water column. Shown: area with megatorches (size of root of torch near bottom exceeds 100 m). Location of megatorches shown in Figs. 3 and 5. Numerals in squares denote indexed series of rooted SSOs.

the total sounding band (Fig. 1). The Seabat 8111 shallow-water multibeam echo sounder installed in 2005 on the R/V *Akademik Nikolai Strakhov* (Geological Institute, RAS) has a total of 101 beams. For each beam, the time of arrival of a bottom signal is detected, which on the basis of model or measured sound velocity profiles is recalculated to depth values. Before the detection procedure, the acoustic signal for each beam is recorded from the moment of emission to the time determined by the total sounding bandwidth. Summation of the same times of beam data of a sampling taken individually starboard and port makes it possible to form a signal similar to an SSS recording (Fig. 2). For a shelf, the duration of the recording represented by the intensity envelope, as a rule, is around 750 ms for a sampling step of 200 μs. Thus, the spatial detail of sonar data from the multibeam echo sounder taking into account the two sides is around 7500 points per emission, which greatly exceeds the number of beams by which depth detection is performed within the limits of the same sounding band.

The usual procedure for processing sonar data is elimination from the recording of the water column interval: slant range correction, after which a mosaic of the scattered signal intensity from a bottom structure is assembled. However, in many cases, the water column contains intense scatterers related either to the discharge of concentrated fluid flows from the bottom into the water column, which speaks to the discrete but noncontinuous character of SSOs as pertains the bottom, or to other causes (Fig. 2). In these cases, it is expedient not to apply standard procedures and limit oneself only to applying the moduli for regulating the intensity. The bottom origin of similar anomalies has been proved many times by many comprehensive studies, e.g. [13]. It is considered established that there is an interrelation of anomalies in the vertical acoustic blanking of seismoacoustic recordings of the sedimentary profile (gas columns) with concentrated fluid flows, which disrupt the coherence of a recording, forming specific shapes of the bottom relief (pockmarks), and gas emissions into the water column in the form of bubble discharge, which scatters the signal of the echo sounder. Also encountered are horizontal anomalies in the illumination of a recording under a gas hydrate sole, which is a fluid flow; these anomalies pass to vertical anomalies at places where this layer is disrupted or degraded. Thus, degassing in this work is understood as passage of a fluid from the bottom, where it forms a specific record in the profiles of unconsolidated sediments, in the form of free bubbles in the water column, the spatial distribution of which is mapped.

The use of a modern multibeam echo sounder makes it possible to obtain a large acoustic recording of the water column in the sounding band (similar to 3D seismic data). At the above-mentioned frequencies, this detection method (water column mapping) generates a large amount of data (several gigabytes per minute). This makes it possible to obtain impressive images of fluid emissions into the water column [11, 12]. These anomalies are also called gas flares, since they are formed, as a rule, owing to signal scattering by gas bubble accumulations [8]. However, this recording method is not used for common reconnaissance surveying when the appearance of flares is not assumed, as well as due to the high memory requirements. The inclusion of 3D recording is expedient in places with confirmed or expected phenomena.

Information on accumulations of scatterers collected by all available methods, including single-beam echo sounders and high-quality profilers, can be collected in a map database [1, 5, 8]. Such databases are of great value for search-related, ecological, and engineering problems.

Therefore, a method has been proposed that is more compact than full 3D visualization in order to form reconnaissance maps with SSO information. Since the sonar mode of a multibeam echo sounder is the integral over the beams for the current time in two halfspaces to starboard and port of the vessel's motion trajectory, exact determination of the location of an SSO in the water column is impossible (Fig. 1). If bottom scattering by an SSS signal is due to the bottom, then the SSO in the water column can theoretically be located anywhere in the space under the vessel's trajectory on a radius equal to the time of the first signal arrival from the bottom (Fig. 1). If the SSO manifests itself in a recording only from one side, this limits its position to the corresponding halfspace (Fig. 2). If the SSO is more or less symmetric in the recording, this means that it is near the central beam. These considerations are related to a cylindrical region under the vessel's trajectory, which has a varying radius of the arrival time of the bottom signal. For times exceeding this value, the amplitudes of the SSO signal drop sharply in comparison to bottom scatterers, and reliable SSO detection in the water column is virtually impossible against the background of higher-amplitude values. This is valid for rootless SSOs having no relation to the bottom. SSO detection in the water column within the radius of the time of first arrival is possible in the case of SSOs like gas flares, which are linked directly to the bottom if the body of the SSO is stretched and it crosses the radius of the time of first arrival when rising to the surface of the bottom (Fig. 1). In this case, we suggest that an SSO with a root is located either in the area of the central beam or one of the sides, with visualization of only the part within the radius of the time of first arrival; however, determination of the exact location of its root is impossible.

In addition to the above-mentioned types of SSOs, a signal subparallel to the bottom is also observed in the water column in the recording, which is related to the contrast boundary of the thermocline related to the hydrophysical properties of water. In a number of cases, this boundary can form a signal comparable in intensity to the bottom signal and can be mapped similarly to the surface of the bottom. Since this signal occurs from inhomogeneities in the water column, in the presented example, its anomalies are comparable in amplitude to rootless SSOs, are superposed on each other, and do not interfere with individual detection of their types.

Taking into account the fundamental limitations in determining the location of SSOs within the sounding band, the following simplified method was realized for compiling maps of such objects. In the RadExPro (Deko-Geofizika, Russia) environment, designed for interpreting seismic data in SEGY format and making it possible to pick the wave field, types are interpreted, the position of the SSO along the vessel's route is picked, and their parameters (height, width) are recorded. The position of an SSO on the time track is not taken into account. Since the detected SSOs formally have an exact linkage only along the route and acrosstrack there is uncertainty, by comparison with the halfwidth of the sounding band, the result of this point picking, which coincides with the vessel's trajectory, can be transferred to a map. Taking into account the variability of SSO manifestations with time (time of day, time of year, action of current, etc.), a similar approach for compiling maps of such objects is quite suitable for revealing key areas with SSOs with subsequent organization of mapping of the water column and full volumetric recording when necessary.

## ANALYSIS OF SSO OBJECTS

Let us consider the example of sonar data from a multibeam echo sounder with manifestations of SSOs (Fig. 2). In the initial part of the sonogram a series of objects is observed with roots in the bottom. The width of the root of object 1 reaches 250 m. Since it is manifested only on the left-hand side, identification of its

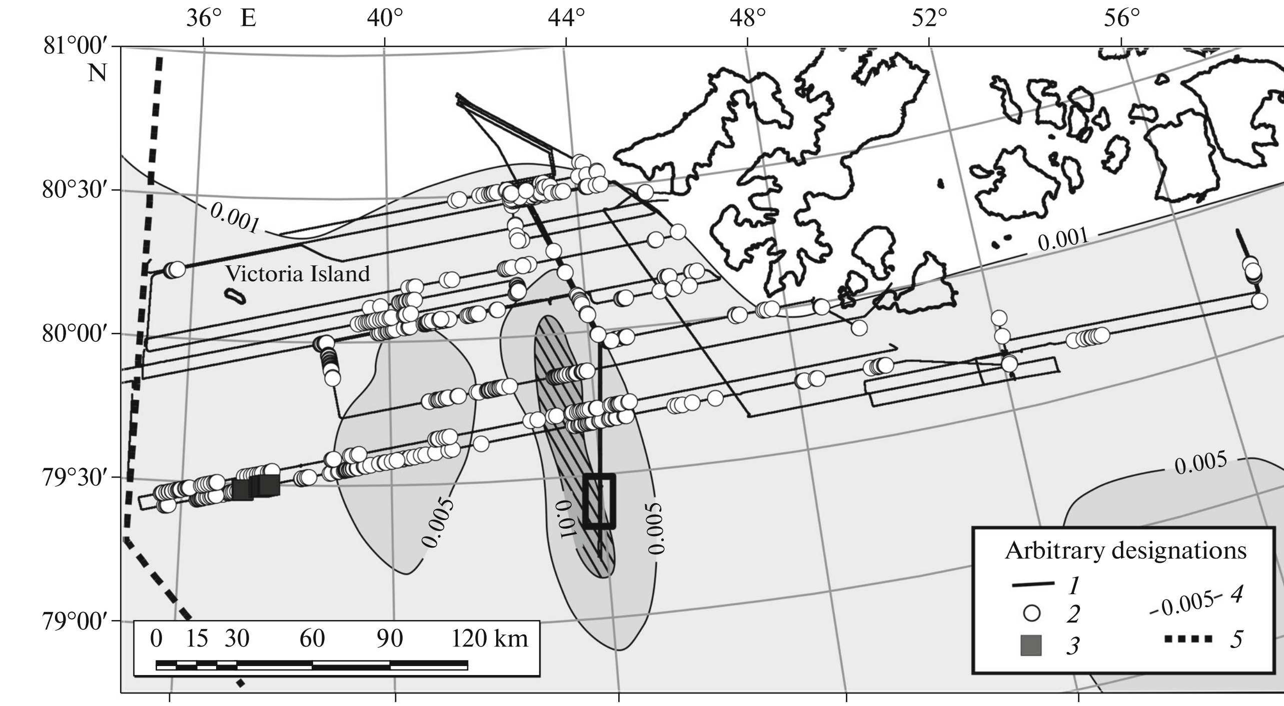


**Fig. 3.** Map of SSOs in northern part of Barents Sea in southwestern framework of Franz Josef Land archipelago according to data of cruise 25 of R/V *Akademik Nikolai Strakhov* (2007; Geological Institute, RAS) and concentration of hydrocarbon gases in bottom sediments [10]. Square shows location of region with pockmarks (Fig. 4). (*1*) Route of cruise 25 of R/V *Akademik Nikolai Strakhov*; (*2*) SSO; (*3*) megaflares ($d > 100$ m); (*4*) isolines of gas concentrations cm$^3$/kg; (*5*) 2011 state boundary.

position with respect to the route of the vessel raises no doubts. Object 2 has a nearly symmetric image in the scattered field from both sides, which speaks to its position directly along the course of the vessel. Objects 3 and 4 are depicted only on the right side. Object 5 assumes weak features from the left side, but is predominantly located on the right side. Finally, object 6 is located only on the right side and has a height almost three times smaller than that of objects 1 and 2, but a similar scattering intensity. The recorded chain of rooted SSOs, many of which have a root width exceeding 100 m, has a psuedoperiodic character of the spatial distribution with a step of around 350 m. The noted SSO features indicate that the detected cluster of megaflares (SSOs with a root width of more than 100 m) is manifested as a linear system located with respect to the route of the vessel from left to right at some angle. This angle can be estimated as follows. Since the height of megaflares at the beginning of the chain is approximately the same, the place when the height of object 6 is shortened to the apparent minimum from object 2 points to outcropping of the flare beyond the limits of the time of first arrival and can be taken as the adjacent side (~1700 m), and the height of object 2, located on the route of the vessel, yields an estimate for the opposite side (~160 m). This gives an angle of about 6°. Note that the estimate was made for a large base, but in reality, megaflares may very likely not be located on a line. Near a chain of megafalres, glacier ploughmarks are observed, but our data contain no direct evidence that degassing was initiated by this phenomenon.

In the central part of the sonogram (Fig. 2), the appearance of rootless SSOs of different shape is observed. These are small scatterers, which may be related to biological objects, as well as narrow and vertically elongated scatters without roots, but which nevertheless may be related to rooted SSOs located far to the side of the sounding band. Large rootless SSOs are observed with amplitudes comparable to megaflares. Transfer of scattering objects by currents is possible. The influence of currents is evidenced by continuous chains of scatterers related to a strong rootless SSO passing to a subhorizontal anomaly lower than the position of the thermocline anomaly. Therefore, the picking of SSOs was done for all large SSOs in order to compare their spatial distribution and geological features, since owing to the dynamics of the medium, accumulations of scatterers can be moved significant distances from the roots—zones of fluid flow discharges from the bottom to the water column.

## COMPARISON OF SSOs AND BOTTOM SEDIMENTS

The SSO distribution differs by the presence of dense spatial clusters of these objects (Fig. 3). Their main manifestation is concentrated in the region of the Franz Victoria tectonic trough located sublongitudinal to the west of Franz Josef Land and breaks off in

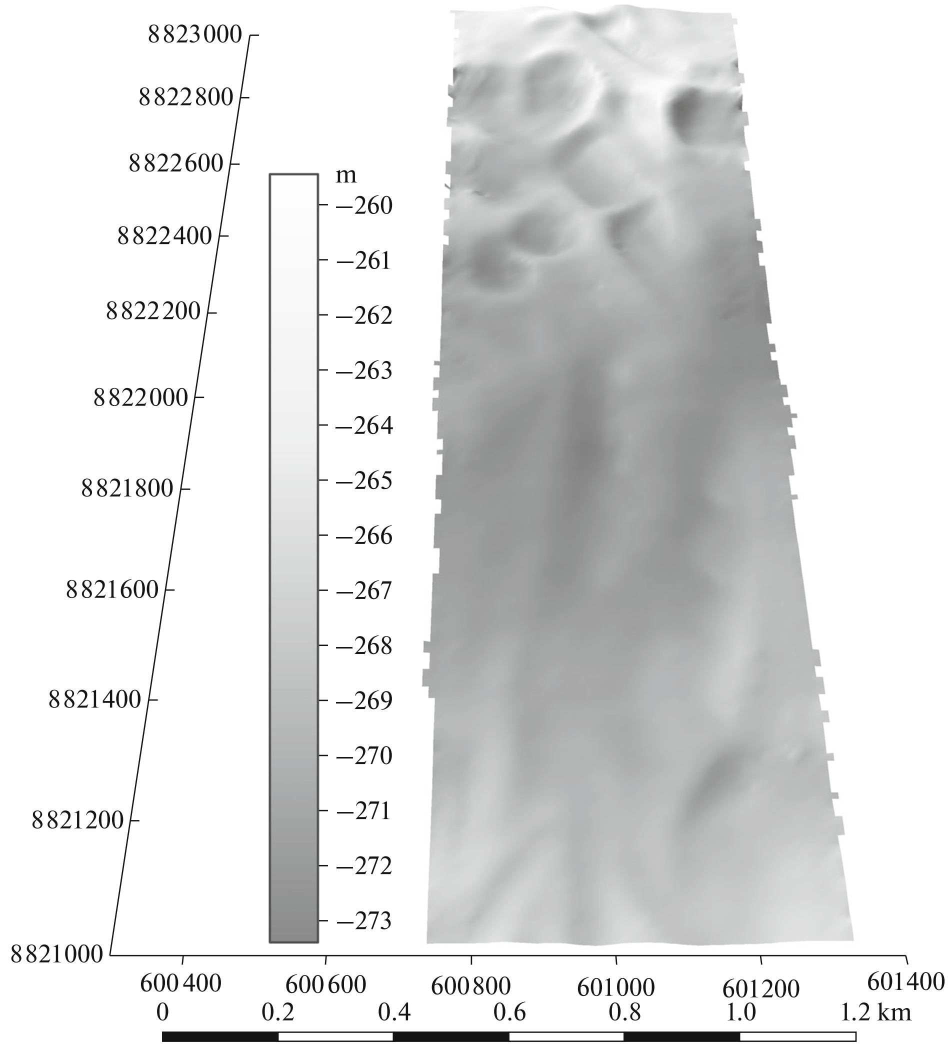


**Fig. 4.** Fragment of bathymetric survey with pockmarks according to data of cruise 28 of R/V *Akademik Nikolai Strakhov* (2011; Geological Institute, RAS). Coordinates, UTM37. Position shown in Figs. 3 and 5.

the western parts of the legs to the arcing rise of Victoria Island. Spatially dense clusters of SSOs are repeated from profile to profile. This is confirmation of the regular manifestation of this phenomenon, which is related to the factor of spatial linkage. Between and along different profiles time passes, and surveying is perhaps carried out at different times of day. This means that spatial clusters of SSOs that correlate from leg to leg are a constantly active phenomenon, at least in a time interval of several days. Exact times of SSO manifestations can be obtained from navigation files. A complete picture of SSO behavior with time can only be obtained by monitoring from a stationary reception location with the tracking of diurnal, seasonal, etc., variations.

The particular density of SSO clusters is manifested in anomalies of hydrocarbon gas concentrations [10] in this part of the water area (Fig. 3). This confirms the interpretation of particular SSOs as degassing objects and not objects of hydrophysical water anomalies related only to water circulation and the biological factor without linkage to the bottom. Anomalous gas concentrations higher that 0.005 cm$^3$/kg [10] are represented by two fields extending along the structures of the Franz Victoria trough. On the southern legs, the SSO clusters coincide well with the configurations of the anomalies. In addition, we can mention the dense SSO fields in the west and north of the operations area beyond the anomalies. This is explained by the incompleteness of the observation network with which the map was compiled [10]: a number of anomalies could have been omitted. However, theoretically, another variant of the time evolution of fluid flows exists, which in this work cannot be studied due to the lack of repeat measurements. Note also that SSOs are encountered predominantly in places where there is no predictive submarine cryolithic zone [7], which may be a local fluid trap that may be degrading in the era of warming [3]. Thus, the preliminary noncontradictory concept of the origin of

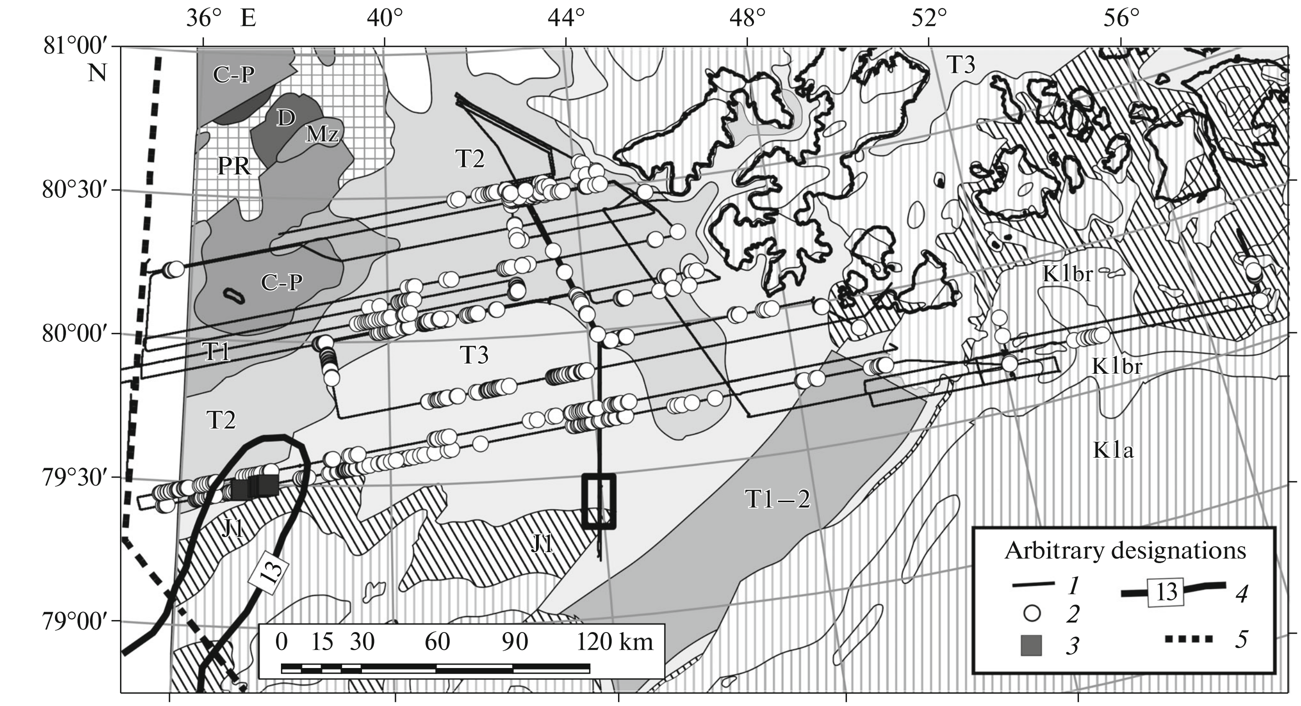


**Fig. 5.** Map of SSOs in northern part of Barents Sea in southwestern framework of Franz Josef Land archipelago according to data of cruise 25 of R/V *Akademik Nikolai Strakhov* (2007; Geological Institute, RAS) and Pre-Quaternary geology of operations area (with simplified 1:1000000 map). Square shows location of region with pockmarks (Fig. 4). (*1*) Route of cruise 25 of R/V *Akademik Nikolai Strakhov*; (*2*) SSO; (*3*) megaflares ($d$ > 100 m); (*4*) isolines Bouguer anomalies (mGal); (*5*) 2011 state boundary.

mapped SSOs is related to their deep origin and degassing from Mesozoic deposits into the water column through Quaternary deposits.

## COMPARISON OF SSOs AND PRE-QUATERNARY GEOLOGY

Besides SSOs in the southern part of the operations area, from the bathymetric data of the echo sounder, a field of gas vents–pockmarks was mapped (Fig. 4), which is located on a gas concentration anomaly of more than 0.01 cm$^3$/kg (Fig. 3). This shows the presence of a direct relationship of the arrival of fluids and phenomena related to their discharge into the water column and with an increase in gas concentration in bottom sediments. The pockmark cluster (Fig. 4) has eight vents with a maximum size of 170 m and depth of up to 7 m. In should be especially noted that such a concentration of pockmarks in this area is a rarity and is manifested at the boundary of Triassic and Jurassic sediments (Fig. 5), which is a regional fluid trap [2]. Bearing in mind the monoclinic character of the bedding of Mesozoic sediments on the north side of the Barents Sea depression and their erosional section near arcing rises, it is possible to conclude that the source of degassing consists of Triassic sequences. Fluids are discharged from them into the water column beyond the contour determined by Jurassic clay sediments. As well, SSOs are absent in the northwest part of the area, where Upper Paleozoic rock sequences are exposed, which limit from below the age interval of rocks from which degassing is observed.

Nearly all SSO clusters according to the data used in the study are located on outcrops of Triassic sediments. Note that in our data there are too few intersections of Jurassic and Triassic contact to reliably confirm linkage of degassing directly to zones covered by a Jurassic fluid trap. However, in the southwestern part of the survey passing parallel and to the north of this contact, we detected megaflares (Figs. 2, 5), which demonstrate, according to the results of operations, the maximum observed discharge of fluids into the water column. According to the data of [4], the operations area is covered by a Quaternary sedimentary cover from 5 to 50 m (in paleochannels), which is an intermediate medium for fluids coming from Early Mesozoic sequences to the water column; it is also a weakly consolidated layer that manifests pockmarks and other indicators of the degassing process that are impossible in the case of ancient consolidated rocks.

According to the data on gravitational Bouguer anomalies [6], in the studied part of the Barents Sea shelf, a local minimum of 13 mGal is distinguished (Fig. 5), which shows the presence of a deep basement depression. Similar minima on the shelf are always an object of increased interest for considerations related to the peculiarities of sediment basins, and in the case of the Barents Sea, to saliferous provinces as well. In our case, the noted local minima of the Bouguer anomaly is related to branching of a Jurassic–Cretaceous rift system [9], which is associated with the accumulation of terrigenous deposits and increased heat flow. It is well seen (Fig. 5) that megaflares are located above the elongated structural basement depression contoured by the 13 mGal isoline. The total fluctuation in the depression in the Bouguer reduction is 20–30 mGal [6]. The concentrated location of megafalres in this area indicates the presence of a gas-containing source of increased productivity.

## CONCLUSIONS

(1) The most intense rooted and rootless SSOs have a degassing origin, and the source of scattering is gas from the discharge of deep focused fluid flows, not from hydrophysical or biological objects.

(2) SSOs are predominantly manifested in places where there are no free gas traps related to the submarine cryolithic zone.

(3) The spatially correlated SSO clusters and pockmarks in the bottom relief form fields related to anomalies of concentrations of hydrocarbon gases in bottom sediments.

(4) Nearly all SSOs and megaflares (rooted SSOs with a root width larger than 100 m) have been detected above an outcropping of Triassic sequences to the bottom, which have been subjected to erosion processes.

(5) Pockmarks and megaflares manifest themselves close to places of contact between Triassic sequences and Jurassic clay deposits, which are represent a regional fluid trap. This points to the possibility of fluid discharges into the water column when trapping sediments are absent.

(6) Megaflares in the water area are located above deep (fluctuations of 20–30 mGal) depressions in the Bouguer anomaly field related to the basement of a Jurassic–Cretaceous rift system, which points to the presence in such a depression of a gas-containing source of increased productivity.

## ACKNOWLEDGMENTS

The authors thank the crew of the R/V *Akademik Nikolai Strakhov* for their selfless work in obtaining under harsh conditions the material used in this paper.

The study was carried out under the topic "Assessment of the Relationship of the Bottom of the Atlantic and Western Arctic Oceans, Deformations of the Sedimentary Cover, Processes of Degassing and Dangerous Geological Phenomena with the Geodynamic State of the Crust and the Upper Mantle" (state registration no. 01201459183); it was also supported by the Russian Foundation for Basic Research (project nos. 15-05-05888, 13-05-12076 ofi_m, 14-05-00122), RAS Presidium program nos. I.18P, I.43P, II.3P, and a Grant in Support of Leading Scientific Schools NSh_5177.2012.5.

## REFERENCES

1. B. V. Baranov, K. A. Dozorova, and A. S. Salomatin, "Flocks of the eastern slope of Sakhalin Island," Vestn. Kamchat. Reg. Assots. Ucheb.-Nauch. Tsentr, Nauki Zemle, No. 2, 31–43 (2011).
2. Yu. A. Volozh, M. P. Antipov, E. V. Shipilov, and N. A. Malyshev, "Complex four-dimensional models of oil-gas sedimentary basins of the eastern margin of the Eastern European Paleozoic continent," in *Fundamental Problems of Geology and Geochemistry of Oil and Gas Complex of Russia* (GEOS, Moscow, 2007), pp. 95–107.
3. L. I. Lobkovskii, S. L. Nikiforov, N. E. Shakhova, et al., "Correlation between the stress-strain state of the Earth's crust in the Eastern Caspian region and zones of earthquake source generation," Dokl. Earth Sci. **449**, 397–401 (2013).
4. E. E. Musatov, "Structure of the Cenozoic cover and neotectonics of the Barents-Kara shelf according to seismoacoustic data," Ross. Zh. Nauk Zemle **1** (2), 157–183 (1998).
5. A. S. Salomatin and V. I. Yusupov, "Acoustic investigations of gas "flares" in the Sea of Okhotsk," Oceanology (Engl. Transl.) **51**, 857 (2011).
6. S. Yu. Sokolov, "Tectonic elements of the Arctic region inferred from small-scale geophysical fields," Geotectonics **43** (1), 18–33 (2009).
7. V. A. Solov'ev and G. D. Ginzburg, "Submarine cryolithozone: distribution forecast," in *Atlas: Geology and Mineral Resources of the Russian Shelves. Russian Arctic Seas* (Nauchnyi Mir, Moscow, 2004), Sheet 3-9.
8. D. V. Chernykh, Candidate's Dissertation in Engineering (Moscow, 2014).
9. E. V. Shipilov, "The tectonic and geodynamic evolution of the continental Arctic margins during young ocean formation," Geotektonika, No. **5**, 26–52 (2004).
10. D. S. Yashin, "Distribution of hydrocarbon gases in bottom sediments," in *Atlas: Geology and Mineral Resources of the Russian Shelves. Russian Arctic Seas* (Nauchnyi Mir, Moscow, 2004), Sheet 1-9.
11. L. Naudts, J. Greinert, Y. Artemov, et al., "Geological and morphological setting of 2778 methane seeps in the Dnepr paleo-delta, northwestern Black Sea," Mar. Geol. **227** (3), 177–199 (2006).
12. T. C. Weber, H. Pena, and M. Jech, "Consecutive acoustic observations of an Atlantic herring school in the Northwest Atlantic," ICES J. Mar. Sci. **66** (6), 1270–1277 (2009).
13. G. K. Westbrook, K. E. Thatcher, E. J. Rohling, et al., "Escape of methane gas from the seabed along the West Spitsbergen continental margin," Geophys. Res. Lett. **36** (15), 1–5 (2009).

*Translated by A. Carpenter*